Kinetic Study on Degradation of Micro-organics by Different UV-based advanced oxidation processes in EfOM Matrix

Donghai Yuan
Beijing University of Civil Engineering and Architecture
Guangyu Liu
Beijing University of Civil Engineering and Architecture
Fei Qi
Beijing Forestry University
Jinggang Wang
Beijing University of Chemical Technology
Yingying Kou (kouyy@bucea.edu.cn)
Beijing University of Civil Engineering and Architecture
Yanqi Cui
Beijing University of Civil Engineering and Architecture
Minghui Bai
Beijing University of Civil Engineering and Architecture
Xinyu Li
Beijing University of Civil Engineering and Architecture

Research Article

Keywords: Effluent organic matter (EfOM), advanced oxidation processes (AOPs), second-order reaction rate constants, sulfate radical, hydroxyl radical

Posted Date: December 6th, 2021

DOI: https://doi.org/10.21203/rs.3.rs-719769/v1

Version of Record: A version of this preprint was published at Environmental Science and Pollution Research on February 10th, 2022. See the published version at https://doi.org/10.1007/s11356-022-19087-0.

Kinetic Study on Degradation of Micro-organics by Different UV-based advanced oxidation processes in EfOM Matrix

Donghai Yuan[a], Guangyu Liu[a], Fei Qi[b], Jinggang Wang[c], Yingying Kou[a,*], Yanqi Cui[a], Minghui Bai[a], Xinyu Li[a]

a Key Laboratory of Urban Stormwater System and Water Environment, Ministry of Education, Beijing University of Civil Engineering and Architecture, Beijing 100044, China

b Beijing Key Lab for Source Control Technology of Water Pollution, College of Environmental Science and Engineering, Beijing Forestry University, Beijing, 100083, PR China

c College of Chemical Engineering，Beijing University of Chemical Technology，Beijing, 100029，PR China

Abstract:

Effluent Organic Matter (EfOM) contains a large number of substances that are harmful to both the environment and human health. To avoid the negative effects of organic matter in EfOM, advanced treatment of organic matter is an urgent task. Four typical oxidants (H_2O_2, PS, PMS, NaClO) and UV-combined treatments were used to treat micro-contaminants in the presence or absence of effluent organic matter (EfOM), because the active radical species produced in these UV-AOPs are highly reactive with organic contaminants. However, the removal efficiency of trace contaminants was greatly affected by the presence of EfOM. The degradation kinetics of two representative micro-contaminants (benzoic acid (BA) and *para*-chlorobenzoic acid(*p*-CBA)) was significantly reduced in the presence of EfOM, compared to the degradation kinetics in its absence. Using the method of competitive kinetics, with BA, *p*-CBA and 1,4-dimethoxybenzene (DMOB) as probes, the radicals ($HO^{\cdot}$, $SO_4^{\cdot-}$, $ClO^{\cdot}$) proved to be the key to reaction species in advanced oxidation processes. UV irradiation on EfOM was not primarily responsible for the degradation of micro-contaminants. The second-order rate constants of the EfOM with radicals were determined to be $(5.027\pm0.643)\times10^2$($SO_4^{\cdot-}$), $(3.192\pm0.153)\times10^4$ ($HO^{\cdot}$) and 1.35×10^6 ($ClO^{\cdot}$) $(mg\text{-}C/L)^{-1}\cdot s^{-1}$. In addition, this study evaluated the production of three radicals based on the concept of R_{ct}, which can better analyze its reaction mechanism.

Key words：Effluent organic matter (EfOM); advanced oxidation processes (AOPs); second-order reaction rate constants; sulfate radical; hydroxyl radical

1. Introduction

Urban sewage contains a large amount of organic matter of various and complex types. Although more than 90% of this organic matter can be effectively removed with conventional biological treatment, some refractory organic residue inevitably remains. These refractory dissolved organic substances remaining in sewage after primary and secondary biochemical treatment are collectively referred to as Effluent Organic Matter (EfOM).(Vigneswaran, 2006) While the concentration of emerging contaminants (ECs) in EfOM is extremely low in the environment,(Rosal et al., 2010) their high stability in wastewater makes them difficult to degrade with conventional biological treatment. (Taoufik et al., 2021) Conventional wastewater treatment processes including coagulation, sedimentation, filtration, and disinfection—can remove only a limited amount of EfOM, and sometimes highly toxic intermediate products are produced during treatment. Advanced Oxidation Process (AOPs) is a new type of high-efficiency pollutant control technology developed in the 1980s.(Hisaindee et al., 2013) Because AOP has strong oxidizing ability and low selectivity to pollutants, and can remove trace amounts of harmful chemicals and refractory organics, it has been widely used in the treatment of contaminated groundwater, especially for the removal of some special trace pollutants in water. With the development of these advanced oxidation processes, in addition to the initial application of $^{\cdot}OH$, other highly reactive free radicals (such as $SO_4^{\cdot-}$, $O_2^{\cdot-}$, $Cl^{\cdot}$, etc.) can undergo electron transfer, or hydrogen addition or substitution, to react with refractory organic matter,(Khan and Adewuyi, 2010) thereby causing chemical bond breakage of the organic matter. It is even possible to directly mineralize the organic matter into carbon dioxide and water.

UV/H_2O_2 is a conventional advanced oxidation process (AOP), based on the production of a hydroxyl radical ($HO^{\cdot}$) (E0 = 2.8 V) via UV/H_2O_2. The major water constituents known to scavenge $HO^{\cdot}$ are EfOM and inorganic species such as carbonate, bicarbonate, nitrite, and bromide ions.(Keen et al., 2014; Wols and Hofman-Caris, 2012) $HO^{\cdot}$ water matrix demand is commonly calculated based on measured concentrations of these compounds and the respective second-order rate constants ($k_{\cdot OH,P}$, $M^{-1}s^{-1}$) for their reaction with $HO^{\cdot}$. The second-order rate constants for the reaction between $HO^{\cdot}$ and EfOM have been reported as 1.0-4.5×10^7 $MC^{-1}s^{-1}$ (And and Fulkersonbrekken†, 1998; Donham et al., 2014; Reisz et al., 2003), and these vary depend on the origin, characteristics, and composition of the EfOM.

An advanced oxidation process based on $SO_4^{\cdot-}$ (E0 = 2.6 V) could be applied as an alternative to those based on a hydroxyl radical ($HO^{\cdot}$) for the remediation of organic pollutants in surface water, groundwater or wastewater.(Hori et al., 2005; Yang et al., 2014) $SO_4^{\cdot-}$ is generated via the activation of peroxymonosulfate (HSO_5^-, PMS) or persulfate ($S_2O_8^{2-}$, PS) by UV, heat or transition metals.(Matta et al., 2011; Zhou et al., 2013)·(Milh et al., 2021) UV/persulfate possesses several advantages, including stability of the precursors (PMS or PS), ease of storage and transportation, high water solubility, versatile activation strategies and a wide operating pH range.(And and Dionysiou, 2004; Das, 2017)· (Giannakis et al., 2021)

UV/Cl is an emerging AOP alternative to the UV/H_2O_2 process, as it produces $HO^{\cdot}$ and reactive chlorine species (RCS). The quantum yields of HOCl and OCl^- by UV photolysis and their absorptivity are reported to be higher than those of H_2O_2.(Feng et al., 2007; Watts and Linden, 2007) Compared to $HO^{\cdot}$, RCS such as $Cl^{\cdot}$, $Cl_2^{\cdot-}$ and $ClO^{\cdot}$ are powerful oxidants, with oxidation potentials of 2.47 V, 2.0 V and 1.5-1.8 V, respectively.(Alfassi et al., 1988; Beitz et al., 1998)

Previous studies have demonstrated the feasibility of adopting advanced oxidation processes to treat micro pollutants.(Cong et al., 2015)·(He et al., 2020) However, data on this topic are still scarce,

especially for UV/oxidant methods for municipal wastewater treatment. In the present work, benzoic acid (BA), *para*-chlorobenzoic acid (*p*-CBA) and 1,4-dimethoxybenzene (DMOB) were chosen as model compounds to investigate the degradation of micro pollutants in UV/H_2O_2, UV/PS, UV/PMS and UV/Cl processes. A kinetic model of UV-based AOPs was established for the degradation of micro pollutants in wastewater, and the second-order rate constants of EfOM with radicals were evaluated.

2. Materials and methods

2.1 Samples and chemicals

Secondary wastewater effluent was obtained from a wastewater treatment plant in Beijing with a capacity of 1,000,000 m^3/d. The municipal sewage was purified by screens, aerated grit chambers and primary settling, and an A^2/O process (anaerobic, anoxic and oxic conditions) and secondary clarification were carried out. The water parameters of the WWTP effluent are listed in Table 1.

Oxone was purchased from Alfa Aesar; H_2O_2 solution (30%), sodium peroxydisulfate (>99%), Sodium hypochlorite (NaClO, ≥8%), and 1,4-dimethoxybenzene (DMOB), benzoic acid (BA; 99%) and *tert*-butyl alcohol (*t*-BuOH>99.5%) were purchased from Sinopharm Chemical Reagent Co., Ltd. (Shanghai, China); *para*-chlorobenzoic acid (*p*-CBA; 98%) was purchased from J&K (Beijing, China); and methanol (>99.9%) and acetonitrile (>99.9%) were purchased from J. T. Baker. Ultrapure deionized water (resistivity >18.0 MΩ*cm) was used in all experiments.

Table 1 Physico-chemical characteristics of raw EfOM

2.2. UV-based advanced oxidation experiment

The photo reactor used for the AOPs was equipped with a Xenon lamp peaking at 254 nm (CEL-HXUV300, Zhongjiao Jinyuan). The average UV fluence rate (E_0) was 1.217 mW cm^{-2}. A 200-mL test solution containing EfOM and 1.0 μM BA, *p*-CBA, or 5.0 μM DMOB was dosed with the oxidant stock solution (PS, PMS, H_2O_2 or NaClO) and simultaneously exposed to UV irradiation at 25±0.2°C. The oxidant dosages of the reaction were 0.588, 1.176, 2.352 and 5.880 mM, respectively. Samples were collected at 10-min intervals for an hour, for further analysis. Reactions of UV/PS, UV/PMS and UV/H_2O_2 were quenched with 100 mM sulfite and UV/Cl reactions were quenched with ascorbic acid at a molar ratio of [ascorbic acid]/[chlorine]=1.5:1. All tests were conducted at least twice. All data plots represent the average of the experimental data of the duplicated test results.

2.3 Analytical methods

High-performance liquid chromatography (HPLC; Waters 2695, USA) was used to determine [BA], [*p*-CBA] and [DMOB] (separation conditions given in Table S1). The column used in the liquid chromatographic analysis of BA, p-CBA and DMOB was a Waters Acquity UPLC BEH C18 (1.7 μm, 2.1×100 mm). The dissolved organic matter in the EfOM was determined using a TOC analyzer (TOC; Shimadzu, Japan), and UV absorbance at 254 nm (UVA_{254}) was measured using a UV/Vis (Evolution 300, Thermo Scientific, USA). Ion chromatography (ICS3000, Dionex Corp., USA) was used to determine [Cl^-], [NO_3^-], and [HPO_3^{2-}]. The separation was finished in an IonPac AS11 column with a

constant gradient mode. The mobile phase eluent was NaOH solution (30.0 mM) and the flow rate was 1.0 mL/min. Before the separation, 25.0 μL of the sample was injected by an autosampler. The pH was measured using a pH meter (S210 Seven Compact, Mettler Toledo).

2.4 Kinetic model of UV-based AOPs

2.4.1 Pseudo-first-order dynamics model

Because UV irradiation showed no effect on the reference compound degradation (shown in Fig.1), and considering that the degradation reaction of the reference compound (R) may be related to the oxidizing properties of the oxidants (PS, PMS and H_2O_2), $SO_4^{\cdot-}$ and $HO^{\cdot}$, the degradation of R can be assumed to follow second-order kinetics:

$$\frac{d[R]}{dt} = k_1[PS][R] + k_2[SO_4^{\cdot-}][R] + k_3[HO^{\cdot}][R] \quad (1)$$

$$\frac{d[R]}{dt} = k_4[PMS][R] + k_5[SO_4^{\cdot-}][R] + k_6[[HO^{\cdot}]][R] \quad (2)$$

$$\frac{d[R]}{dt} = k_7[H_2O_2][R] + k_8[[HO^{\cdot}]][R] \quad (3)$$

where k_i is the second-order rate constant of the reaction of PS, PMS, H_2O_2, $SO_4^{\cdot-}$ and $HO^{\cdot}$ with R. It is known that the minimum concentration of PS, PMS or H_2O_2 is 0.588 mM, and it can be assumed that the BA and *p*-CBA concentration is 1.0 μM [Oxidant]≫[R]. In order to simplify Eqs. (1)-(3), k_{app} is introduced:

$$\frac{d[R]}{dt} = k_{app}[R] \quad (4)$$

Then, the integral is transformed to

$$-ln\frac{[R]}{[R]_0} = k_{app}t \quad (5)$$

where k_{app} is the apparent reaction rate constant (s^{-1}), and $[R]_0$ (mM) and [R] (mM) represent the concentrations of R at the reaction times at *0* and *t*, respectively.

2.4.2 Determination of second-order rate constants of $HO^{\cdot}$ and EfOM

To quantify the reactivity of EfOM with $HO^{\cdot}$, the second-order rate constants ($k_{HO^{\cdot},EfOM}$, $MC^{-1}s^{-1}$) between $HO^{\cdot}$ and EfOM were determined based on the competition kinetics method using BA, *p*-CBA and MeOH (or *t*-BuOH) in UV/H_2O_2, since the reaction rate constants of BA, *p*-CBA and MeOH (or *t*-BuOH) with $HO^{\cdot}$ were known.

$$k_R^{app} = k_{HO^{\cdot},R} \times [HO^{\cdot}]_{SS} = k_{HO^{\cdot},R} \times \frac{\alpha_{HO^{\cdot}}}{k_{HO^{\cdot},EfOM}[EfOM] + k_{HO^{\cdot},MeOH/t\text{-}BuOH}[MeOH/t\text{-BuOH}] + k_{HO^{\cdot},R}[R] + k_{HO^{\cdot},H_2O_2}[H_2O_2]} \quad (6)$$

Then,

$$\frac{1}{k_R^{app}} = \frac{k_{HO^{\cdot},\ MeOH/t\text{-}BuOH}}{k_{HO^{\cdot},R} \times \alpha_{HO^{\cdot}}}[\text{MeOH/t-BuOH}] + \frac{k_{HO^{\cdot},EfOM}[EfOM] + k_{HO^{\cdot},R}[R] + k_{HO^{\cdot},H_2O_2}[H_2O_2]}{k_{HO^{\cdot},R} \times \alpha_{HO^{\cdot}}} \quad (7)$$

where k_R^{app} is the apparent degradation rate constant of R (s^{-1}), and $k_{HO^{\cdot},R}$ is the second-order rate constant for the reaction between $HO^{\cdot}$ and compound R ($M^{-1}s^{-1}$). $[HO^{\cdot}]_{ss}$ is the steady-state concentration of $HO^{\cdot}$ (M), and $\alpha_{HO^{\cdot}}$ is the formation rate of $HO^{\cdot}$ (M s^{-1}).

In order to eliminate the capture of hydroxyl radicals by inorganic ions in the EfOM and determine the concentrations of Cl^-, NO_3^- and HPO_3^{2-}, we introduced the parameter β:

$$\beta = k_9 \times [Cl^-] + k_{10} \times [NO_3^-] + k_{11} \times [HPO_3^{2-}] \quad (8)$$

where k_9, k_{10}, k_{11} are the second-order rate constants of $HO^\cdot$ with Cl^-, NO_3^- and HPO_3^{2-}, respectively.(Alfassi et al., 1988; Buxton et al., 1988; Herrmann et al., 1999)

Bringing β into Eq. 7 gives

$$\frac{1}{k_R^{app}} = \frac{k_{HO^\cdot,\ \mathrm{MeOH/t\text{-}BuOH}}}{k_{HO^\cdot,\ R} \times \alpha_{HO^\cdot}} [\mathrm{MeOH}/t\text{-BuOH}] + \frac{k_{HO^\cdot,EfOM}[EfOM] + k_{HO^\cdot,R}[R] + k_{HO^\cdot,H_2O_2}[H_2O_2] + \beta}{k_{HO^\cdot,R} \times \alpha_{HO^\cdot}} \quad (9)$$

2.4.3 Determination of second-order rate constants of $SO_4^{\cdot-}$ and EfOM

Similar to calculating the secondary reaction rate of $HO^\cdot$ with EfOM, the second-order rate constant ($k_{SO_4^{\cdot-},EfOM}$,$M^{-1}\ s^{-1}$) of the reaction between EfOM and $SO_4^{\cdot-}$ is the same as above, using BA, *p*-CBA and MeOH (or *t*-BuOH) in the UV/PS system and UV/PMS system.

$$\gamma = k_{12} \times [Cl^-] + k_{13} \times [NO_3^-] + k_{14} \times [HPO_3^{2-}] \quad (10)$$

$$\frac{1}{k_R^{app}} = \frac{k_{SO_4^{\cdot-},\ MeOH/\text{t-BuOH}}}{k_{SO_4^{\cdot-},\ R} \times \alpha_{SO_4^{\cdot-}}} [MeOH/t\text{-}BuOH] + \frac{k_{SO_4^{\cdot-},EfOM}[EfOM] + k_{SO_4^{\cdot-},R}[R] + k_{SO_4^{\cdot-},PS/PMS}[PS/PMS] + \gamma}{k_{SO_4^{\cdot-},R} \times \alpha_{SO_4^{\cdot-}}} \quad (11)$$

where k_{12}, k_{13} and k_{14} are the second-order rate constants of $SO_4^{\cdot-}$ with Cl^-, NO_3^- and HPO_3^{2-}, respectively; k_R^{app} is the apparent degradation rate constant of R(s^{-1}); $k_{SO_4^{\cdot-},R}$ is the second-order rate constant for the reaction between $SO_4^{\cdot-}$ and compound "R;" and $\alpha_{SO4^{\cdot-}}$ is the formation rate of $SO_4^{\cdot-}$ ($M\ s^{-1}$).

2.4.4 Determination of second-order rate constants of $ClO^\cdot$ and EfOM

The second-order rate constants ($k_{ClO\bullet}$) for the reaction of $ClO^\cdot$ with EfOM were determined by competition kinetics between EfOM and a reference compound of 1,4-dimethoxybenzene (DMOB), which was selected to be the reference compound because of its available k value with $ClO^\cdot$ of 2.1×10^9 $M^{-1}\ s^{-1}$. The pseudo-first order rate constant (k') of DMOB varied depending on the presence or absence of EfOM, as shown in Eq 12:

$$\frac{k'_{R-0}}{k'_{R-i}} = 1 + \frac{k_{ClO\bullet,\mathrm{EfOM}}}{k_{ClO\bullet,R}} \times \frac{[\mathrm{EfOM}]_0}{[\mathrm{R}]_0} \quad (12)$$

where $[EfOM]_0$ and $[R]_0$ represent the initial concentrations of the EfOM and the DMOB respectively; k'_{R-0} and k'_{R-i} represent the $k'$of the reference compound (DMOB) in the absence and presence of EfOM, respectively; and $k_{ClO\bullet,EfOM}$ and $k_{ClO\bullet,R}$ represent the second-order rate constants of $ClO^\cdot$ reacting with the EfOM and the DMOB, respectively. (Guo et al., 2018)

3. Results and discussion

3.1 Removal efficiencies of reference compounds in EfOM by UV/ oxidants

Fig. 1 Degradation profile of probes (BA and *p*-CBA) in UV-based AOP: (A) UV/ H_2O_2, (B) UV/PS, (C) UV/PMS, (D) UV/Cl; 1-BA, 2-*p*CBA.

Reaction conditions: [BA or *p*-CBA] =1.0 μM, E_0= 1.217 mW cm^{-2}, solution pH= 7.9

Fig. 1 compares the degradation of BA (or *p*-CBA) by the UV/H_2O_2, UV/PS, UV/PMS and UV/Cl systems at different oxidant concentrations in EfOM and ultrapure water. BA and *p*-CBA are commonly used as radical probe compounds in UV-based AOPs because they have high reactivity with radicals, especially with $HO^{\cdot}$ and $SO_4^{\cdot-}$. On the whole, probe compounds have the best degradation effect in ultrapure water, as the concentration of oxidants is 0.588 mM background in different oxidation systems. The degradation rates of BA in the UV/H_2O_2, UV/PS, UV/PMS, and UV/Cl systems were 86.07%, 79.05%, 56.94% and 54.91%, respectively, and the degradation rates of *p*-CBA in the UV/H_2O_2, UV/PS, UV/PMS and UV/Cl systems were 69.42%, 50.17%, 44.77% and 60.02%, respectively. It can be concluded that the AOPs had the potential to degrade the contaminants. The pseudo-first-order reaction rate constants for BA were 4.90×10^{-4}, 3.54×10^{-4}, 2.31×10^{-4} and 2.14×10^{-4} cm^2 mJ^{-1} in the UV/H_2O_2, UV/PS, UV/PMS and UV/Cl systems, respectively, and the pseudo-first-order reaction rate constants for p-CBA were 2.73×10^{-4}, 1.55×10^{-4}, 1.60×10^{-4} and 2.58×10^{-4} cm^2 mJ^{-1} in the UV/H_2O_2, UV/PS, UV/PMS and UV/Cl systems, respectively (as shown in Table S2). It can be seen that the reaction rates of BA were higher than those of *p*-CBA in the UV/H_2O_2, UV/PS and UV/PMS systems, indicating that the reaction mechanisms between the two probes and the radicals ($HO^{\cdot}$ and $SO_4^{\cdot-}$) differed. The reaction rate was opposite in the UV/Cl system, where the degradation of *p*-CBA in ultrapure water was significantly faster than the degradation of BA, while the opposite results were obtained in the EfOM background.

The degradation of BA and *p*-CBA in the secondary effluent organic matter by UV alone had little effect. The efficiency of the degradation rate of the two probes under UV irradiation showed a significant relationship with the molar absorption coefficient (ε) and quantum yield (Φ)(Kwon et al., 2015). As the concentration of oxidants increased, the degradation efficiency of the probe compounds also increased, indicating that the concentration of radicals increased. But this increase was not continuous. It can be seen that when the concentration reached 5.880 mM, the degradation efficiency was basically the same as for the concentration of 2.352 mM. For example, the pseudo-first-order reaction rate constant for BA was 1.13×10^{-4} cm^2 mJ^{-1} with a PS concentration of 2.235 mM, and the reaction rate constant for BA was 1.15×10^{-4} cm^2 mJ^{-1} with a concentration of 5.880 mM in the UV/PS system. The reason for this difference is that the concentration of the micro-contaminant was limited, in the wastewater. When the concentration of free radicals reaches a certain value, the reaction is saturated. Therefore, an oxidant concentration of 2.352 mM was selected for the next experiment.

The degradation rate of the UV/H_2O_2 system was higher than for other processes. For example, the pseudo-first-order reaction rate constants for BA were 1.64×10^{-4}, 1.13×10^{-4}, 1.56×10^{-4}, and 1.57×10^{-4} cm^2 mJ^{-1} in UV/H_2O_2, UV/PS, UV/PMS and UV/Cl systems, respectively, with a 2.352-mM concentration of oxidants in the presence of EfOM. In the UV/H_2O_2 system, the major oxidant was the hydroxyl radical ($HO^{\cdot}$); the reaction is shown below (Reaction 1). H_2O_2 is decomposed to generate a powerful oxidant HO• under the irradiation of ultraviolet light and to trigger free radical chain reactions. PS is stable at room temperature, and the UV led to the cleavage of the O-O bond of PS and generated two $SO_4^{\cdot-}$ molecules (Reaction 2), which was efficient at degrading the probes. Compared to PDS, PMS has a shorter bond, and more energy is required to cleave the peroxide bond and generate $HO^{\cdot}$ and $SO_4^{\cdot-}$(Reaction 3). The redox potential of $SO_4^{\cdot-}$ is equal to or even better than $HO^{\cdot}$ (Ghauch and Tuqan, 2012) but $SO_4^{\cdot-}$ is more selective than $HO^{\cdot}$ in degrading the contaminants, which may have led to the lower degradation rate in the UV/PMS and UV/PDS than in the UV/H_2O_2 system. In the UV/Cl system, there are several kinds of radicals, such as $OH^{\cdot}$, $Cl^{\cdot}$, $ClO^{\cdot}$, and $Cl_2^{\cdot-}$, that are responsible for degrading the probes in the effluent organic matter (Reactions 5-10).

In particular, a large amount of $SO_4^{\cdot-}$ is transformed to $HO^{\cdot}$ under basic conditions (Reaction 4). In the presence of p-CBA, the conditions are more acidic compared to those in the presence of BA, indicating that the degradation rate of BA is higher than that of p-CBA. Besides, the main reaction of BA with $HO^{\cdot}$ is the direct attack of the $HO^{\cdot}$ on the aromatic ring to form a hydroxy-substituted compound.(Singla et al., 2004) However, the reaction of $SO_4^{\cdot-}$ with BA first leads to the formation of a radical cation followed by hydrolysis, to form 4-hydroxybenzoic acid (HBA).(Ying-Hong et al., 2011a) This is why the BA degrades faster in UV/H_2O_2 than in the UV/PS or UV/PMS systems.

Table 2 Reactions involved in the different UV-based advanced oxidation processes

In the UV/PS system, the degradation efficiencies of BA and *p*-CBA were 40.66% and 26.85%, respectively, at the concentration of 5.880 mM in the presence of EfOM. Under the same conditions, the degradation efficiencies under UV/PMS were 44.04% and 28.35%, respectively. Mahdi-Ahmed(Mahdi-Ahmed and Chiron, 2014) and Minhwan Kwon(Lee et al., 2018) also found that the removal rate of the probe compound in the UV/PS process is higher than that of the UV/PMS process in ultrapure water, whereas the UV/PMS process has a higher removal rate of the probe compound than the UV/PS process in wastewater from a sewage treatment plant. Guan's research results proved that UV/PMS significantly enhances the degradation of BA in the pH range of 9-11, while the concentration of PMS has little effect.(Ying-Hong et al., 2011b)

By comparing the degradation results in ultrapure water and EfOM, we observed that the degradation of the probe compound by different oxidant concentrations in EfOM is not as effective as in ultrapure water. It can be reasonably inferred that this is most likely because the organic matter contained in EfOM has a trapping effect on the radicals, which leads to different results in the degradation of the probe compound by different oxidation systems. Therefore, we elected to use the competition kinetics method to calculate the second-order rate constants of EfOM and radicals.

3.2 Contribution of different radicals to contaminant degradation in EfOM

To demonstrate the $HO^{\cdot}$ and $SO_4^{\cdot-}$ reactivity with the EfOM, the second-order rate constants between radicals and the EfOM were determined based on the competition kinetics method using probes (BA, *p*-CBA) and inhibitors (MeOH, *t*-BuOH) in the UV/PS, UV/PMS and UV/H_2O_2 systems. The initial concentration of MeOH (or *t*-BuOH) was varied from 0 mM to 0.10 mM, and the initial concentrations of probes and oxidants were fixed at 1.0 μM and 2.352 mM, respectively. The introduction of MeOH and *t*-BuOH significantly inhibited the degradation of probes in UV/PS, UV/PMS and UV/H_2O_2 compared to results in the absence of quencher, indicating that $HO^{\cdot}$ and $SO_4^{\cdot-}$ are the main reactive oxidizing species. In the sulfate radical systems, when 0.1 mM of radical scavenger was applied, the removal efficiency of BA and *p*-CBA was reduced by about 30% in the presence of MeOH (Fig. 2); while almost no BA or *p*-CBA decrease was observed with the addition of *t*-BuOH (Table S3 and Fig. 3). These results indicated that $SO_4^{\cdot-}$ was the predominant reactive species in the UV/PS and UV/PMS systems, a result consistent with a study by Osburn.(Osburn et al., 2009) Fig. 4 and Fig. 5 show the experimental results of the competition kinetics for the calculation of the second-order rate constants. Due to the reactivity of $ClO^{\cdot}$, the second-order rate constant for the reaction between $ClO^{\cdot}$ and EfOM was determined using DMOB as a reference compound with varying EfOM concentrations, which react with $ClO^{\cdot}$ at the second-order rate constant of 2.1×10^9 M^{-1} s^{-1} (Alfassi et al., 1988) (Fig. 6).

Fig. 2 Pseudo primary degradation of added MeOH in EfOM (includes BA and *p*-CBA)
Reaction conditions：$[BA]_0 = [p\text{-}CBA]_0 = 1.0$ μM，$[PS]_0 = [PMS]_0 = [H_2O_2]_0 = 2.352$ mM，$[MeOH]_0 = 0$,10，20，50 和 100Mm
Fig. 3. Pseudo primary degradation of added t-BuOH in EfOM (includes BA and p-CBA)
Reaction conditions：$[BA]_0 = [p\text{-}CBA]_0 = 1.0$ μM，$[PS]_0 = [PMS]_0 = [H_2O_2]_0 = 2.352$ mM $[t\text{-}BuOH]_0 = 0$,10，20，50 和 100 μM
Fig. 4 Reciprocal of the apparent rate constants for BA and *p*CBA *vs.* MeOH concentrations: (a) UV/H_2O_2 system; (b) UV/PS system; (c) UV/PMS system
Reaction conditions: $[BA \text{ or } p\text{-}CBA]_0 = 1.0$ μM, $[oxidant]_0 = 2.352$ mM, $E_0 = 1.217$ mW cm^{-2}, solution pH=7.9
Fig. 5 Competitive dynamics of BA and p-CBA at different tert-butanol concentrations
Reaction conditions：$[BA]_0 = [p\text{-}CBA]_0 = 1.0$ μM，$[PS]_0 = [PMS]_0 = [H_2O_2]_0 = 2.352$ mM $[t\text{-}BuOH]_0 = 0$，10、20、50 和 100 μM
Fig. 6 Competition kinetic plot for $ClO^{\bullet}$ reaction with EfOM using 1,4-dimethoxybenzene (DMOB) as a reference compound.
Reaction conditions: $[chlorine]_0 = 2.353$ mM, $[DMOB]_0 = 5.0$ μM, $[EfOM]_0 = 0$, 1444, 3344, 5244, 6384 μg L^{-1}

Table S6 lists the second-order rate constants determined for the reactions between the EfOM and radicals. To verify the method and rate constants determined in this study, both probes and inhibitors were measured in each of the different oxidation systems. The second-order rate constant of EfOM and $HO^{\cdot}$ was determined to be (3.192±0.153) $\times 10^4$ $(mg\text{-}C/L)^{-1}$ s^{-1}, which is within the commonly reported range of second-order rate constants. These rate constants are similar to the 10^3-10^{11} $M^{-1}s^{-1}$ range of second-order rate constants for the reaction of organics with $HO^{\cdot}$ presented in the literature: these are compared with other studies in Table S5. The results of Yang and NAGARNAIK P M—3.3×10^4 $(mg\text{-}C/L)^{-1}$ $s^{-1}$and (7.1±0.81) $\times 10^4$ $(mg\text{-}C/L)^{-1}$ s^{-1}, respectively(Nagarnaik and Boulanger, 2011; Yang et al., 2016)—are very similar to our findings. In the sulfate radical-mediated oxidation system, the error of the determined rate constant ($k_{SO_4^{\cdot-},EfOM}$ =(5.027±0.643)×10^2 ($(mg\text{-}C/L)^{-1}$ s^{-1}) in this study was small, indicating the reliability of the measurement method. And compared with the other studies shown in Table S4, Yang's samples of EfOM were isolated from RO Brine A by solid-phase extraction, and contain a large amount of chloride ions, exceeding the probe compounds concentration by 1300- to 2300-fold. They observed that $SO_4^{\cdot-}$ can be converted to more selective halogen and carbonate radicals, resulting in a wider range of degradation efficiencies among the contaminants.(Yang et al., 2016) Zhou measured the absolute rate constants of the reaction of $SO_4^{\cdot-}$ with four types of organic matter: two fulvic acids and two types of lake organic matter, and their results were close to those in our research.(Zhou et al., 2017) The differences in the organic matter contained in the effluent are the main cause of the difference in research results, and are also related to the choice of secondary biochemical reaction process.

Because the UV/Cl process is an emerging advanced oxidation process (AOP) used for the degradation of micropollutants, there has been little research on the secondary reaction rate constant of $ClO^{\cdot}$ reacting with different substances in aqueous systems. The second-order kinetic rate constant for EfOM with a chlorooxyl radical was calculated to be 1.35×10^6 $(mg\text{-}C/L)^{-1}$ s^{-1} in this research. This value is two orders of magnitude higher than that from EfOM from the Tai Cang wastewater treatment plant in Shanghai—1.83×10^4 $(mg\text{-}C/L)^{-1}$ s^{-1}. (Guo et al., 2018) Guo(Guo et al., 2017) researched simulated drinking water prepared by spiking NOM in pure water (1mg L^{-1}), and the k value of the organic matter with $ClO^{\cdot}$ was 4.52×10^4 $(mg\text{-}C/L)^{-1}$ s^{-1}. The difference in k values between the organic matter of different sources and

$ClO^{\cdot}$ may be due to the different components of the wastewater.

3.3 Calculating the radical production rate in EfOM

It is well known that a wastewater matrix such as carbonate species and EfOM affects the removal efficiency of a reference compound (R) in a radical-mediated system.(Rosenfeld and Linden, 2007; Yuan et al., 2011) Von Gunten and Linden introduced the concept of R_{ct} to model these complex matrix effects in different AOPs.(Elovitz et al., 2000b; Rosenfeld and Linden, 2007) The R_{ct} concept, defined as the experimentally determined radical exposure per UV fluence for a given water matrix and initial oxidants concentration, can characterize the effectiveness of the UV/oxidant AOPs within a specific water matrix.(Elovitz et al., 2000a) To quantify the scavenging effect of the EfOM, $R_{HO^{\cdot},UV}$, and $R_{SO_4^{-\cdot},UV}$ were calculated with Eqs. (12) and (13), respectively:

$$R_{SO_4^{-\cdot},UV} = \frac{k^{\mathrm{D,EfOM}}_{R,UV/P(M)S^{-}} k^{\mathrm{D,EfOM}}_{R,UV}}{k_{R,SO_4^{-\cdot}}} = \frac{\int_0^t [SO_4^{-\cdot}]\mathrm{dt}}{H} \quad (13)$$

$$R_{HO^{\cdot},UV} = \frac{k^{\mathrm{D,EfOM}}_{R,UV/H_2O_2/PMS^{-}} k^{\mathrm{D,EfOM}}_{R,UV}}{k_{R,HO^{\cdot}}} = \frac{\int_0^t [HO^{\cdot}]\mathrm{dt}}{H} \quad (14)$$

where $k^{D,EfOM}_{R,UV}$ is the apparent first-order rate constant (s^{-1}) of R destruction in EfOM under UV conditions, and $k^{\mathrm{D,EfOM}}_{R,UV/\mathrm{Oxidants}}$ is the apparent first-order rate constant (s^{-1}) of R degradation in the UV/oxidants system in the presence of EfOM. The superscript "D" indicates that the value is fluence-based. UV fluence (H in the unit of mJ cm^{-2}) is simply the product of E_0 and t. The detailed calculation method refers to the study of Gao et al. (Gao et al., 2019)

Figure 7 displays the first-order degradation kinetics of probe compounds as a function of applied UV fluence at EfOM in the different UV/oxidant systems. The decay is first order with UV fluence, with only one kinetic regime throughout. Through Figure 7, we can use Formulas (13) and (14) to calculate the data in Table S7, which illustrates the R_{ct} values of $SO_4^{-\cdot}$ and $HO^{\cdot}$ to BA or *p*–CBA degradation in a UV/PS, UV/PMS or UV/H_2O_2 system. When BA is used as a probe, UV/PS produces an $SO_4^{-\cdot}$ value of 9.42×10^{-14} M s cm^2 mJ^{-1}, and UV/PMS produces two kinds of radicals —$HO^{\cdot}$ and $SO_4^{-\cdot}$—2.64×10^{-14} M s cm^2 mJ^{-1} and 1.30×10^{-13} M s cm^2 mJ^{-1}, of which the one mainly producing $SO_4^{-\cdot}$ accounted for 83.1%. The $HO^{\cdot}$ produced by UV/H_2O_2 was 2.78×10^{-14} M s cm^2 mJ^{-1}. And using *p*-CBA as a probe, UV/PS produced $SO_4^{-\cdot}$ of 1.94×10^{-13} M s cm^2 mJ^{-1}, while $HO^{\cdot}$ and $SO_4^{-\cdot}$ in UV/PMS produced fluxes of 1.78×10^{-14} M s cm^2 mJ^{-1} and 2.48×10^{-13} M s cm^2 mJ^{-1}, and the proportion of $SO_4^{-\cdot}$ was 93.3%. The $HO^{\cdot}$ produced by UV/H_2O_2 was 2.66×10^{-15} M s cm^2 mJ^{-1}. By comparing the scavenging effects of different oxidation systems on the two probes, it can be observed that the $SO_4^{-\cdot}$ produced by UV/PS and UV/PMS was more effective. Although the degradation of EfOM is more rapid in UV/H_2O_2, $SO_4^{-\cdot}$ is more reactive with specific contaminants than $HO^{\cdot}$, in the degradation of specific pollutants.

In general, the most useful application of the R_{ct} parameter may be in calculating the scavenging properties of the wastewater matrix(Rosenfeld and Linden, 2007) and assessing the potential of $SO_4^{-\cdot}$-based AOPs in wastewater treatment systems. We used a method of experimentally assessing the exposures of radicals in UV/oxidant AOPs. This parameter can be used to compare water-matrix effects on such UV/oxidant AOPs, to compare the model oxidation of environmental pollutants of concern during AOP treatments in different types of water. This parameter can also be useful in comparing efficiencies among several AOPs.

Fig. 7 Pseudo-first-order degradation of BA (or p-CBA) by different oxidant concentrations in EfOM and ultrapure water

Reaction conditions: [BA or *p*-CBA] =1.0 μM, E_0= 1.217 mW cm^{-2}, solution pH= 7.9

Conclusions

The effect of UV-based advanced oxidation processes (UV/H_2O_2, UV/PS, UV/PMS, UV/Cl) in degrading probes (BA, p-CBA, DMOB) in the absence or presence of EfOM was investigated. Direct UV photolysis is not effective because of the low quantum yield. With the addition of oxidants (H_2O_2, PS, PMS, NaClO), the removal rate was largely improved due to the formation of $HO^{\cdot}$, $SO_4^{\cdot-}$ and $ClO^{\cdot}$. As the concentration of oxidants increases, the degradation efficiency of the probe compounds also increases. The oxidant concentration of 2.352 mM was selected to degrade the probes. Due to its different degradation mechanism, the reaction rate of BA was higher than *p*-CBA in the UV/H_2O_2, UV/PS and UV/PMS systems. The degradation rates of BA decreased in the order UV/H_2O_2>UV/PS>UV/PMS>UV/Cl, whereas the order of the *p*-CBA degradation rates was UV/H_2O_2>UV/Cl >UV/PS>UV/PMS in ultrapure water. With the competition kinetics method using a probe (BA, *p*-CBA) and inhibitors (MeOH, *t*-BuOH) in the UV/PS, UV/PMS and UV/H_2O_2 systems, results indicated that $HO^{\cdot}$ and $SO_4^{\cdot-}$ are the principal radicals. The second-order rate constants of the EfOM with radicals were determined to be $(3.192\pm0.153)\times10^4$ M s cm^2 mJ^{-1} ($HO^{\cdot}$), $(5.027\pm0.643)\times10^2$ M s cm^2 mJ^{-1} ($SO_4^{\cdot-}$) and 1.35×10^6 M s cm^2 mJ^{-1} ($ClO^{\cdot}$). With the introduction of R_{ct} to the wastewater, results indicated that $SO_4^{\cdot-}$ was the principal radical in the UV/PMS and UV/PS systems, and $HO^{\cdot}$ is the principal radical in UV/H_2O_2.

Declarations

Ethics approval and consent to participate

Not applicable

Consent for publication

Not applicable

Availability of data and materials

All data generated or analyzed during this study are included in this published article and its supplementary information files.

Competing interests

The authors declare that they have no competing interests.

Funding

This work is supported by National Water Pollution Control and Management Technology Major Project (2018ZX07110005), the National Natural Science Foundation of China (51578037), the Guangxi Province Technology Major Project (AA17202032), the Scientific Research Program of Beijing

Municipal Education Commission (KM201610016001) and the Fundamental Research Funds for Beijing University of Civil Engineering and Architecture (X18288, X18289 and X20137).

Authors' contributions

DY: Writing-Editing & Review, Funding acquisition; **GL**: Data curation, Writing-Original draft preparation; **FQ:** Writing-Editing & Review, Conceptualization; **JW:** Writing-Review, Visualization; **YK:** Writing-Editing & Review, Funding acquisition; **YC**: Investigation; **MB**: Visualization; **XL**: Methodology

References

Alfassi, Z. B., Huie, R. E., Mosseri, S., and Neta, P. (1988). Kinetics of one-electron oxidation by the ClO radical. International Journal of Radiation Applications & Instrumentation.part C.radiation Physics & Chemistry **32**, 3888-3891.

And, G. P. A., and Dionysiou, D. D. (2004). Radical Generation by the Interaction of Transition Metals with Common Oxidants. Environmental Science & Technology **38**, 3705.

And, P. L. B., and Fulkersonbrekken†, J. (1998). Nitrate-Induced Photolysis in Natural Waters: Controls on Concentrations of Hydroxyl Radical Photo-Intermediates by Natural Scavenging Agents. Environmental Science & Technology **32**, 3004-3010.

Beitz, T., Bechmann, W., and Mitzner, R. (1998). Investigations of Reactions of Selected Azaarenes with Radicals in Water. 2. Chlorine and Bromine Radicals. Journal of Physical Chemistry A **102**, 6766-6771.

Buxton, G. V., Greenstock, C. L., Helman, W. P., and Ross, A. B. (1988). Critical Review of rate constants for reactions of hydrated electrons, hydrogen atoms and hydroxyl radicals (· OH/ O− in Aqueous Solution. Journal of Physical and Chemical Reference Data **17**, 513-886.

Cong, J., Wen, G., Huang, T., Deng, L., and Ma, J. (2015). Study on enhanced ozonation degradation of para-chlorobenzoic acid by peroxymonosulfate in aqueous solution. Chemical Engineering Journal **264**, 399-403.

Das, T. N. (2017). Reactivity and role of SO5•- radical in aqueous medium chain oxidation of sulfite to sulfate and atmospheric sulfuric acid generation. Journal of Physical Chemistry A **105**, 9142-9155.

Donham, J. E., Rosenfeldt, E. J., and Wigginton, K. R. (2014). Photometric hydroxyl radical scavenging analysis of standard natural organic matter isolates. Environmental Science Processes & Impacts **16**, 764-769.

Elovitz, M. S., Gunten, U. V., and Kaiser, H. P. (2000a). Hydroxyl Radical/Ozone Ratios During Ozonation Processes. II. The Effect of Temperature, pH, Alkalinity, and DOM Properties. Ozone Science & Engineering **22**, 123-150.

Elovitz, M. S., von Gunten, U., and Kaiser, H.-P. (2000b). Hydroxyl Radical/Ozone Ratios During Ozonation Processes. II. The Effect of Temperature, pH, Alkalinity, and DOM Properties. Ozone Science & Engineering **22**, 123-150.

Feng, Y., Smith, D. W., and Bolton, J. R. (2007). Photolysis of aqueous free chlorine species (HOCl and OCl–) with 254 nm ultraviolet light. Journal of Environmental Engineering & Science **6**, 179-180.

Gao, L., Minakata, D., Wei, Z., Spinney, R., Dionysiou, D. D., Tang, C. J., Chai, L., and Xiao, R. (2019). Mechanistic Study on the Role of Soluble Microbial Products in Sulfate Radical-Mediated Degradation of Pharmaceuticals. Environ Sci Technol **53**, 342-353.

Ghauch, A., and Tuqan, A. M. (2012). Oxidation of bisoprolol in heated persulfate/H2O systems: Kinetics and products. Chemical Engineering Journal **183**, 162-171.

Giannakis, S., Lin, K.-Y. A., and Ghanbari, F. (2021). A review of the recent advances on the treatment of industrial wastewaters by Sulfate Radical-based Advanced Oxidation Processes (SR-AOPs). Chemical Engineering Journal **406**.

Guo, K., Wu, Z., Shang, C., Yao, B., Hou, S., Yang, X., Song, W., and Fang, J. (2017). Radical Chemistry and Structural Relationships of PPCP Degradation by UV/Chlorine Treatment in Simulated Drinking Water. Environmental Science & Technology **51**, 10431.

Guo, K., Wu, Z., Yan, S., Yao, B., Song, W., Hua, Z., Zhang, X., Kong, X., Li, X., and Fang, J. (2018). Comparison of the UV/chlorine and UV/H2O2 processes in the degradation of PPCPs in simulated drinking water and wastewater: Kinetics, radical mechanism and energy requirements. Water Res **147**, 184-194.

He, D. Q., Zhang, Y. J., Pei, D. N., Huang, G. X., Liu, C., Li, J., and Yu, H. Q. (2020). Degradation of benzoic acid in an advanced oxidation process: The effects of reducing agents. J Hazard Mater **382**, 121090.

Herrmann, H., Ervens, B., Nowacki, P., Wolke, R., and Zellner, R. (1999). A chemical aqueous phase radical mechanism for tropospheric chemistry. Chemosphere **41**, 633-634.

Hisaindee, S., Meetani, M. A., and Rauf, M. A. (2013). Application of LC-MS to the analysis of advanced oxidation process (AOP) degradation of dye products and reaction mechanisms. Trends in Analytical Chemistry **49**, 31-44.

Hori, H., Yamamoto, A., Hayakawa, E., Taniyasu, S., Yamashita, N., Kutsuna, S., Kiatagawa, H., and Arakawa, R. (2005). Efficient decomposition of environmentally persistent perfluorocarboxylic acids by use of persulfate as a photochemical oxidant. Environmental Science & Technology **39**, 2383-2388.

Keen, O. S., Mckay, G., Mezyk, S. P., Linden, K. G., and Rosario-Ortiz, F. L. (2014). Identifying the factors that influence the reactivity of effluent organic matter with hydroxyl radicals. Water Research **50**, 408-419.

Khan, N. E., and Adewuyi, Y. G. (2010). Absorption and Oxidation of Nitric Oxide (NO) by Aqueous Solutions of Sodium Persulfate in a Bubble Column Reactor. Industrial & Engineering Chemistry Research **49**, 8749-8760.

Kwon, M., Kim, S., Yoon, Y., Jung, Y., Hwang, T.-M., Lee, J., and Kang, J.-W. (2015). Comparative evaluation of ibuprofen removal by UV/H2O2 and UV/S2O82− processes for wastewater treatment. Chemical Engineering Journal **269**, 379-390.

Lee, D., Kwon, M., Ahn, Y. T., Jung, Y., Nam, S. N., Choi, I. H., and Kang, J. W. (2018). Characteristics of intracellular algogenic organic matter and its reactivity with hydroxyl radicals. Water Research **144**, 13.

Mahdi-Ahmed, M., and Chiron, S. (2014). Ciprofloxacin oxidation by UV-C activated peroxymonosulfate in wastewater. Journal of Hazardous Materials **265**, 41-46.

Matta, R., Tlili, S., Chiron, S., and Barbati, S. (2011). Removal of carbamazepine from urban wastewater by sulfate radical oxidation. Environmental Chemistry Letters **9**, 347-353.

Milh, H., Yu, X., Cabooter, D., and Dewil, R. (2021). Degradation of ciprofloxacin using UV-based advanced removal processes: Comparison of persulfate-based advanced oxidation and sulfite-based advanced reduction processes. Sci Total Environ **764**, 144510.

Nagarnaik, P. M., and Boulanger, B. (2011). Advanced oxidation of alkylphenol ethoxylates in aqueous systems. Chemosphere **85**, 854-860.

Osburn, C. L., Retamal, L., and Vincent, W. F. (2009). Photoreactivity of chromophoric dissolved organic matter transported by the Mackenzie River to the Beaufort Sea. Marine Chemistry **115**, 10-20.

Reisz, Erika, Schmidt, Winfried, Schuchmann, HeinzPeter, Sonntag, and Von, C. (2003). Photolysis of ozone in aqueous solutions in the presence of tertiary butanol. Environmental Science & Technology **37**, 1941-1948.

Rosal, R., Rodríguez, A., Perdigónmelón, J. A., Petre, A., Garcíacalvo, E., Gómez, M. J., Agüera, A., and Fernándezalba, A. R. (2010). Occurrence of emerging pollutants in urban wastewater and their removal through biological treatment followed by ozonation. Water Research **44**, 578-588.

Rosenfeld, E. J., and Linden, K. G. (2007). The ROH,UV concept to characterize and the model uv/H202 process in natural waters. Environmental Science & Technology **41**, 2548-53.

Singla, R., Ashokkumar, M., and Grieser, F. (2004). The mechanism of the sonochemical degradation of benzoic acid in aqueous solutions. Research on Chemical Intermediates **30**.

Taoufik, N., Boumya, W., Achak, M., Sillanpaa, M., and Barka, N. (2021). Comparative overview of advanced oxidation processes and biological approaches for the removal pharmaceuticals. J Environ Manage **288**, 112404.

Vigneswaran, S. (2006). Effluent Organic Matter (EfOM) in Wastewater: Constituents, Effects, and Treatment. Critical Reviews in Environmental Science & Technology **36**, 327-374.

Watts, M. J., and Linden, K. G. (2007). Chlorine photolysis and subsequent OH radical production during UV treatment of chlorinated water. Water Research **41**, 2871-2878.

Wols, B. A., and Hofman-Caris, C. H. (2012). Review of photochemical reaction constants of organic micropollutants required for UV advanced oxidation processes in water. Water Research **46**, 2815-2827.

Yang, Y., Pignatello, J. J., Ma, J., and Mitch, W. A. (2014). Comparison of halide impacts on the efficiency of contaminant degradation by sulfate and hydroxyl radical-based advanced oxidation processes (AOPs). Environmental Science & Technology **48**, 2344.

Yang, Y., Pignatello, J. J., Ma, J., and Mitch, W. A. (2016). Effect of matrix components on UV/H 2 O 2 and UV/S 2 O 8 2− advanced oxidation processes for trace organic degradation in reverse osmosis brines from municipal wastewater reuse facilities. Water Research **89**, 192-200.

Ying-Hong, G., Jun, M., Xu-Chun, L., Jing-Yun, F., and Li-Wei, C. (2011a). Influence of pH on the formation of sulfate and hydroxyl radicals in the UV/peroxymonosulfate system. Environmental science & technology **45**.

Ying-Hong, G., Jun, M., Xu-Chun, L., Jing-Yun, F., and Li-Wei, C. (2011b). Influence of pH on the formation of sulfate and hydroxyl radicals in the UV/peroxymonosulfate system. Environmental Science & Technology **45**, 9308.

Yuan, F., Hu, C., Hu, X., Wei, D., Chen, Y., and Qu, J. (2011). Photodegradation and toxicity changes of antibiotics in UV and UV/H2O2 process. Journal of Hazardous Materials **185**, 1256-1263.

Zhou, L., Sleiman, M., Ferronato, C., Chovelon, J.-M., and Richard, C. (2017). Reactivity of sulfate radicals with natural organic matters. Environmental Chemistry Letters **15**, 733-737.

Zhou, L., Zheng, W., Ji, Y., Zhang, J., Zeng, C., Zhang, Y., Wang, Q., and Yang, X. (2013). Ferrous-activated persulfate oxidation of arsenic(III) and diuron in aquatic system. Journal of Hazardous Materials **263**, 422-430.

Figures

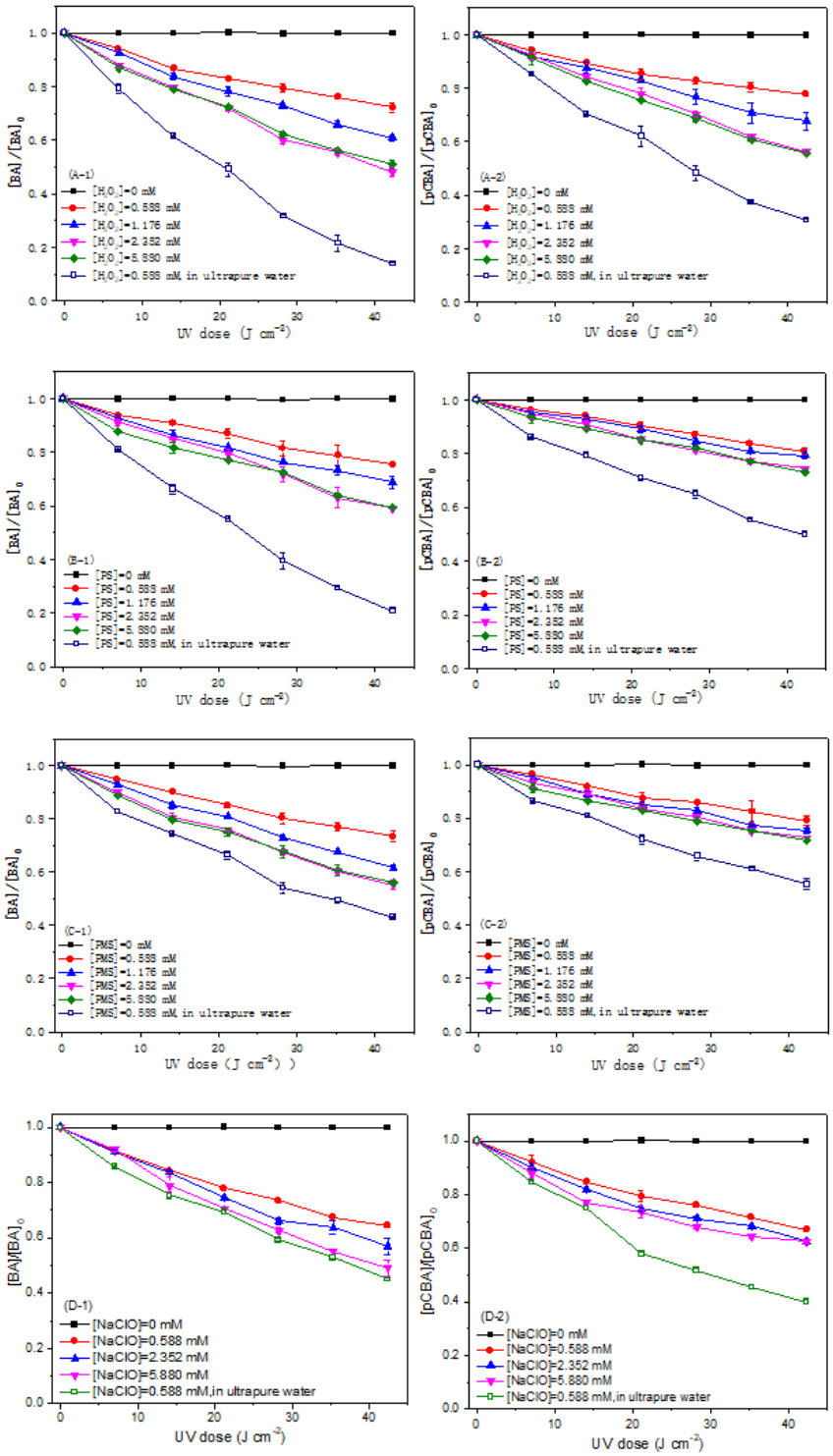

Figure 1

Degradation profile of probes (BA and p-CBA) in UV-based AOP: (A) UV/ H2O2, (B) UV/PS, (C) UV/PMS, (D) UV/Cl; 1-BA, 2-pCBA.

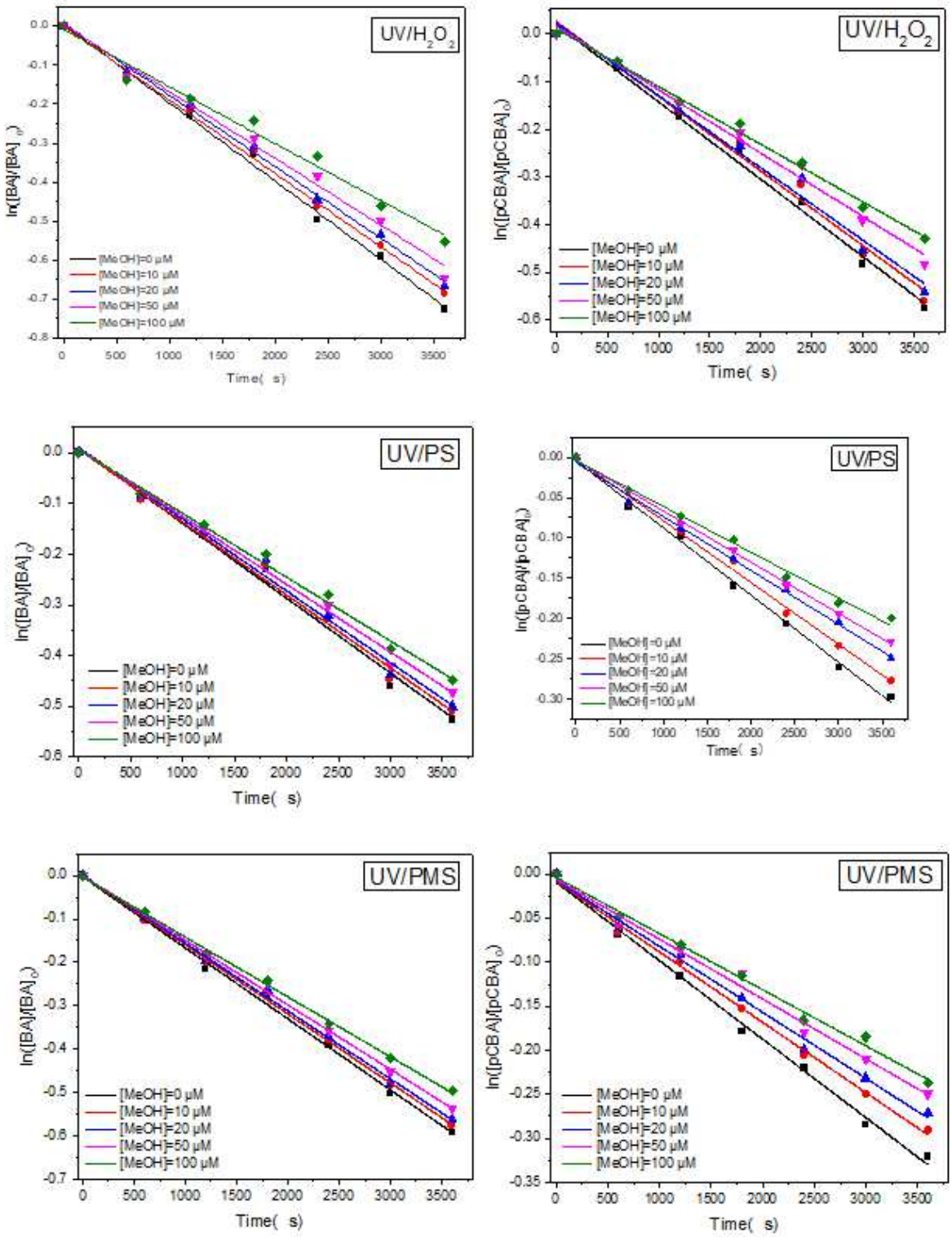

Figure 2

Pseudo primary degradation of added MeOH in EfOM (includes BA and p-CBA) Reaction conditions：[BA] 0 = [p-CBA] 0 = 1.0 μM；[PS] 0 = [PMS] 0 = [H2O2] 0 = 2.352 mM； [MeOH] 0 = 0,10，20，50，100Mm

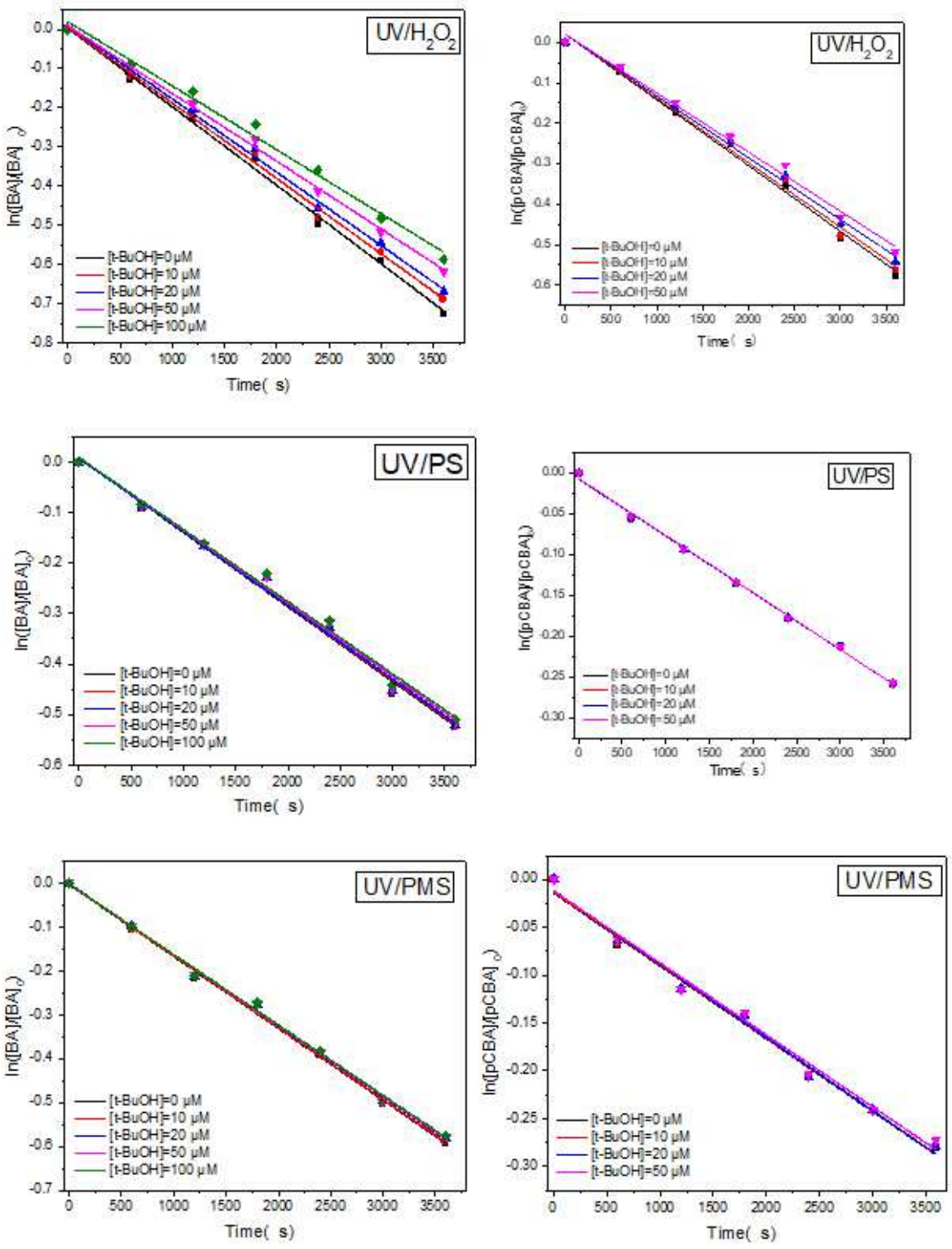

Figure 3

Pseudo primary degradation of added t-BuOH in EfOM (includes BA and p-CBA) Reaction conditions [BA]0 = [p-CBA]0 = 1.0 μM [PS]0 = [PMS]0 = [H2O2]0 = 2.352 mM [t-BuOH]0 = 0,10 20 50 100 μM

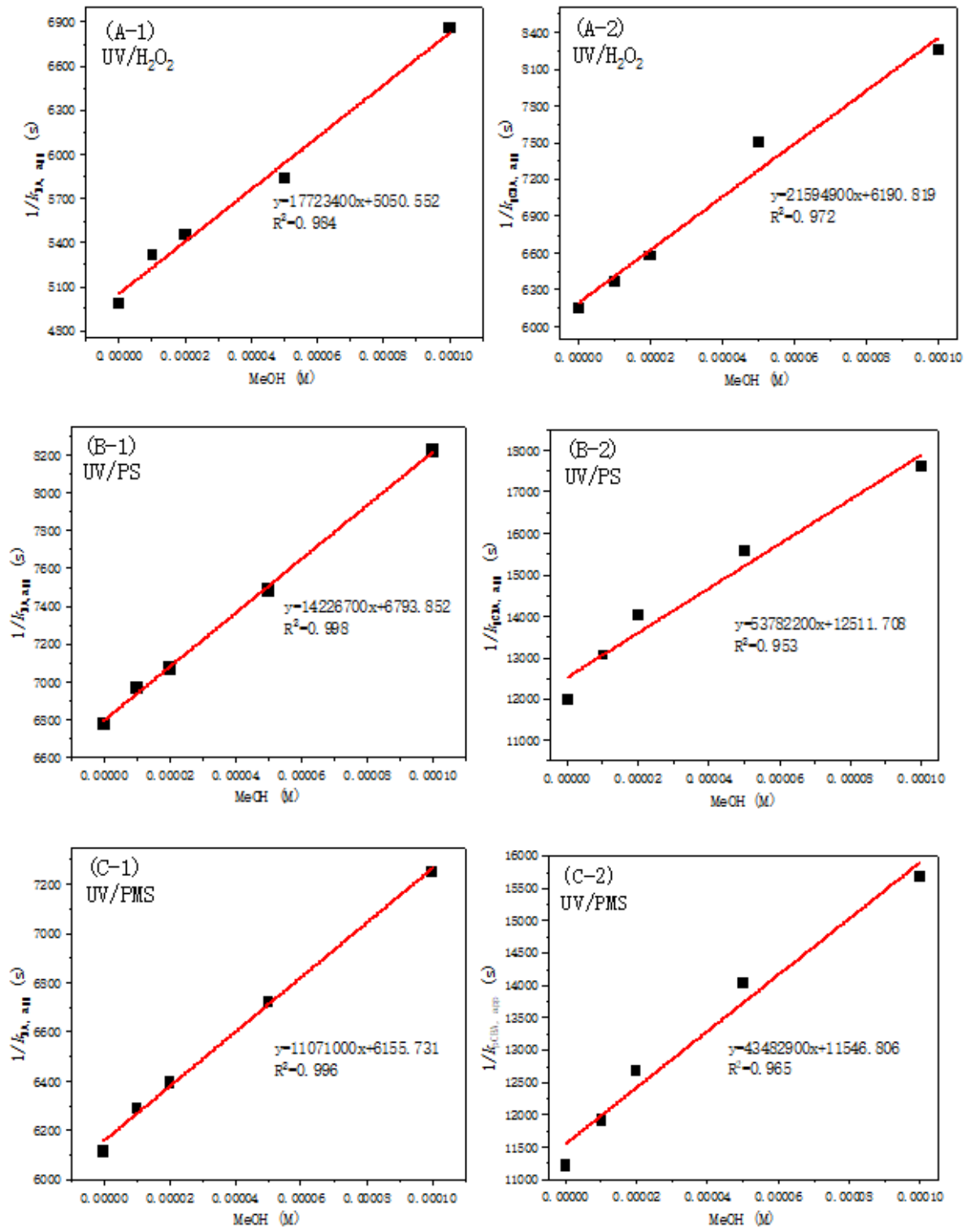

Figure 4

Reciprocal of the apparent rate constants for BA and pCBA vs. MeOH concentrations: (a) UV/H2O2 system; (b) UV/PS system; (c) UV/PMS system Reaction conditions: [BA or p-CBA]0 =1.0 μM, [oxidant]0=2.352 mM, E0=1.217 mW cm-2, solution pH=7.9

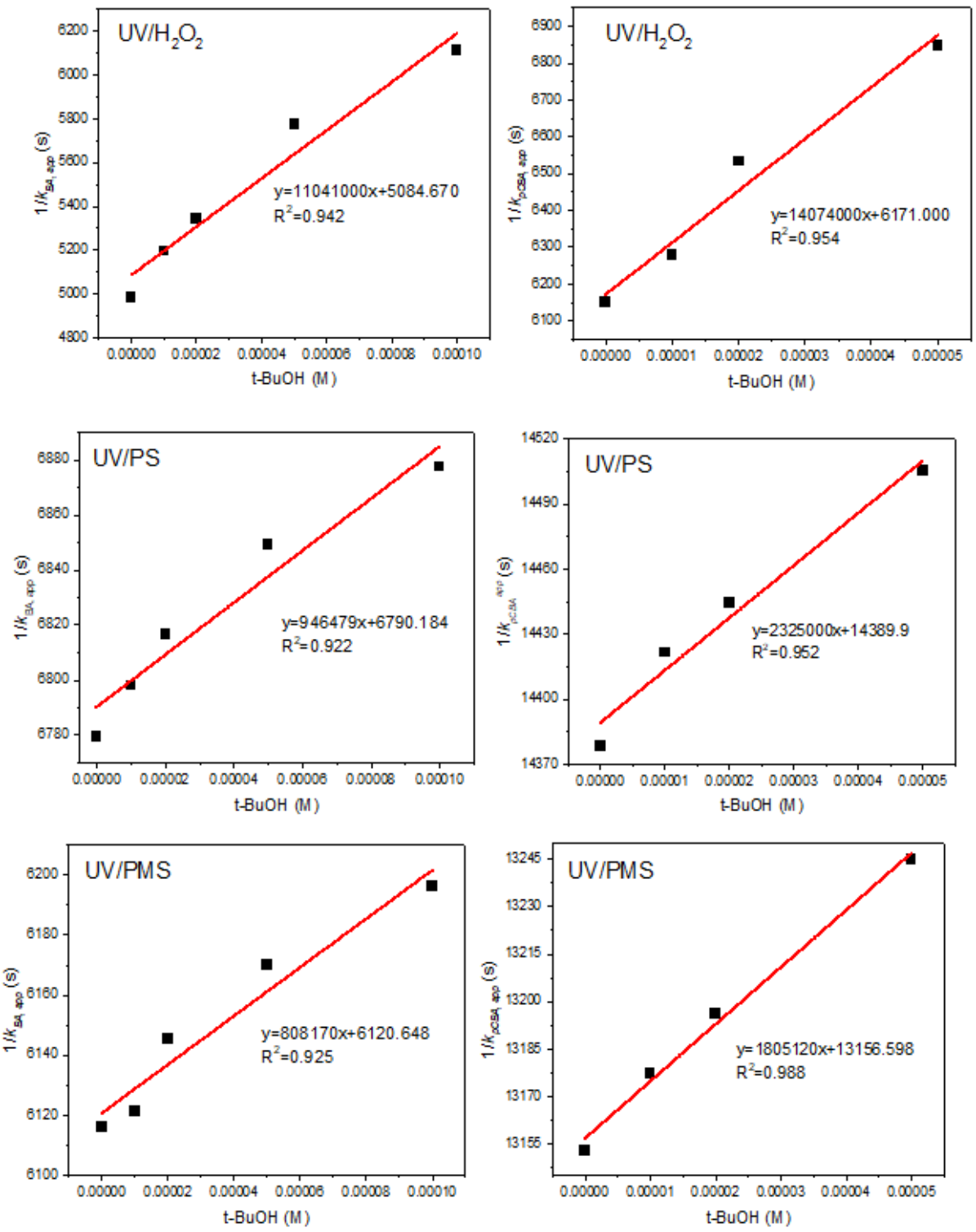

Figure 5

Competitive dynamics of BA and p-CBA at different tert-butanol concentrations Reaction conditions：[BA]0 = [p-CBA]0 = 1.0 μM；[PS]0 = [PMS]0 = [H2O2]0 = 2.352 mM [t-BuOH]0 = 0、10、20、50、100 μM

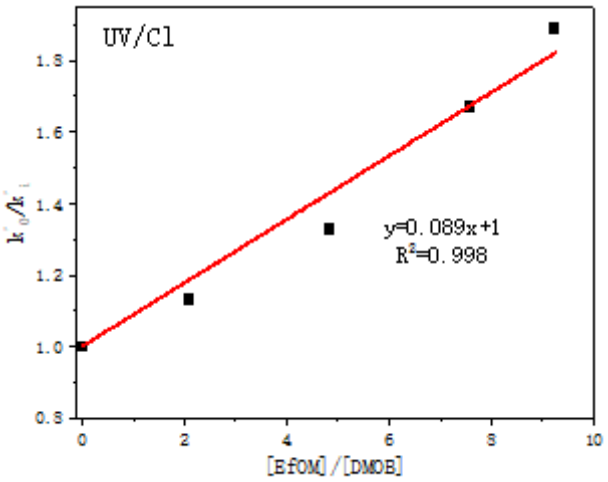

Figure 6

Competition kinetic plot for ClO• reaction with EfOM using 1,4-dimethoxybenzene (DMOB) as a reference compound. Reaction conditions: [chlorine]0 =2.353 mM, [DMOB]0 =5.0 μM, [EfOM]0 =0, 1444, 3344, 5244, 6384 μg L-1

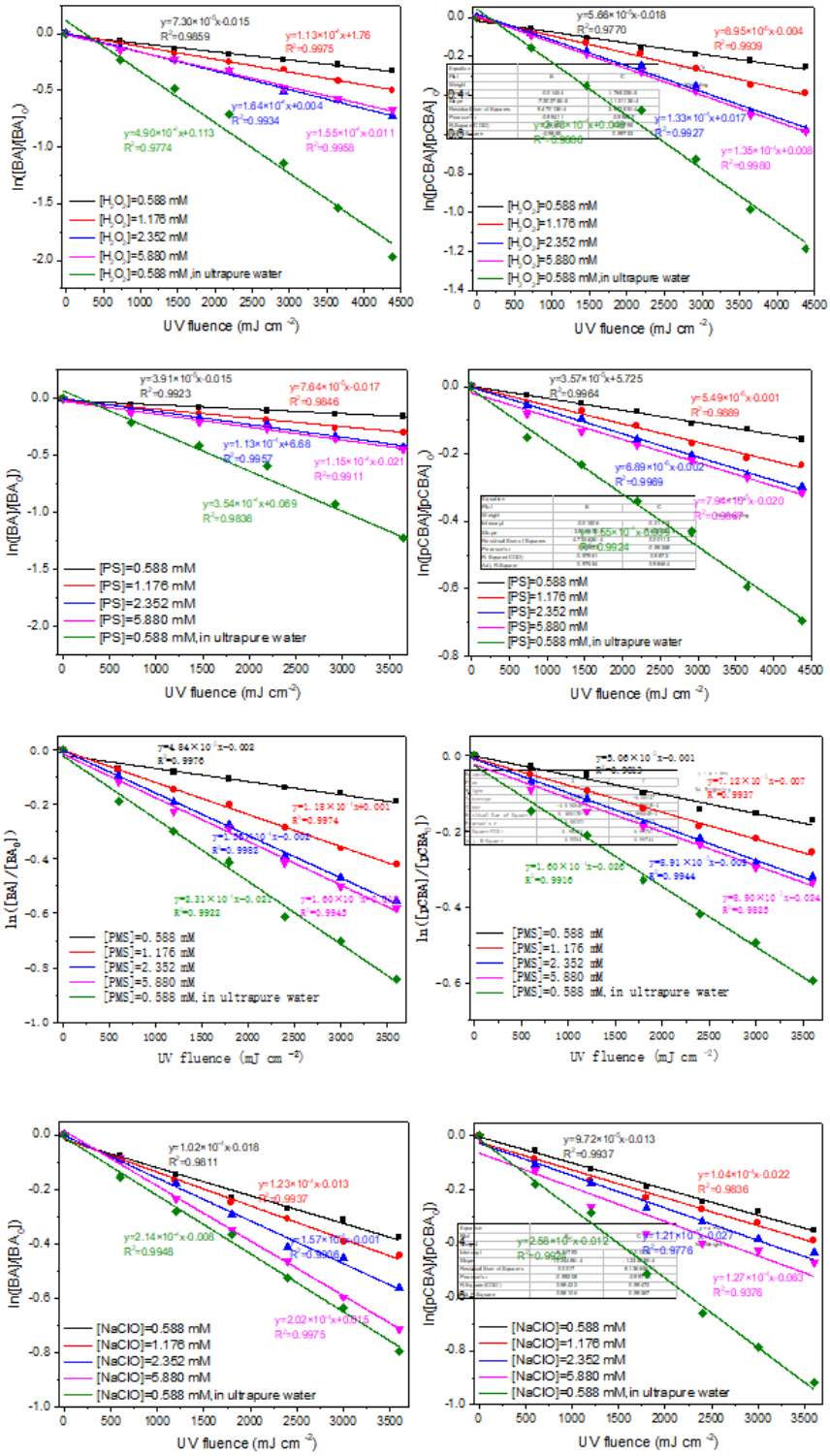

Figure 7

Pseudo-first-order degradation of BA (or p-CBA) by different oxidant concentrations in EfOM and ultrapure water Reaction conditions: [BA or p-CBA] =1.0 μM, E0= 1.217 mW cm-2, solution pH= 7.9

Supplementary Files

This is a list of supplementary files associated with this preprint. Click to download.

- SupplementaryMaterial.docx